JACS
JOURNAL OF THE AMERICAN CHEMICAL SOCIETY

Communication

pubs.acs.org/JACS

Water-Dispersible, Responsive, and Carbonizable Hairy Microporous Polymeric Nanospheres

Weicong Mai,[†] Bin Sun,[†] Luyi Chen,[†] Fei Xu,[†] Hao Liu,[†] Yeru Liang,[†] Ruowen Fu,[†] Dingcai Wu,*[,†] and Krzysztof Matyjaszewski*[,‡]

[†]Materials Science Institute, Key Laboratory for Polymeric Composite and Functional Materials of Ministry of Education, School of Chemistry and Chemical Engineering, Sun Yat-sen University, Guangzhou 510275, P. R. China

[‡]Department of Chemistry, Carnegie Mellon University, Pittsburgh, Pennsylvania 15213, United States

Supporting Information

ABSTRACT: Multifunctionalization of microporous polymers is highly desirable but remains a significant challenge, considering that the current microporous polymers are generally hydrophobic and nonresponsive to different environmental stimuli and difficult to be carbonized without damage of their well-defined nanomorphology. Herein, we demonstrate a facile and versatile method to fabricate water-dispersible, pH/temperature responsive and readily carbonizable hairy microporous polymeric nanospheres based on combination of the hyper-cross-linking chemistry with the surface-initiated atom transfer radical polymerization (SI-ATRP). The hyper-cross-linking creates a highly microporous core, whereas the SI-ATRP provides diverse functionalities by surface grafting of hairy functional blocks. The as-prepared materials present multifunctional properties, including sensitive response to pH/temperature, high adsorption capacity toward adsorbates from aqueous solution, and valuable transformation into well-defined microporous carbon nanospheres because of hybrid of carbonizable core and thermo-decomposable protection shell. We hope this strategy could promote the development of both functional microporous polymers and advanced hairy nanoparticles for multipurpose applications.

Over the past few decades, design and fabrication of various nanoporous materials, including porous carbons,[1] porous silicas,[2] porous metal oxides,[3] metal−organic[4] and covalent organic[5] frameworks, and amorphous porous polymers,[6] have attracted increasing interest for both fundamental research and practical applications. Porous polymers combine the superiority of porous materials and functional polymers. They have well-defined porosity, high surface area, lightweight, tunable surface chemistry and are easily processable.[6f] With such attributes, porous polymers are extensively used in diverse fields including energy,[7] adsorption,[6c,d,8] separation,[9] medicine,[10] and catalysis.[11] In recent years, significant progress has been achieved in synthetic methods, structural, compositional, and topological control over polymeric framework and control of pore structure including pore size, pore geometry, and pore surface in porous polymer field. Among various porous polymers, microporous polymers, defined as polymeric materials with pores smaller than 2 nm,[6f] have been one of the most fertile arenas in materials science. Because of their extremely developed surface area and small pore size, microporous polymers are widely utilized in gas storage, adsorption, separation, and catalysis. However, the polymeric frameworks for most microporous polymers generally comprise a highly cross-linked hydrophobic network which restricts their use in various aqueous media. Therefore, it is very challenging to prepare inherently water-dispersible microporous polymers. Moreover, introduction of multifunctionalities represents another significant challenge for microporous polymers. For example, to the best of our knowledge, microporous polymers with sensitive response to the environmental stimuli such as pH and temperature have not yet been reported. In addition, it is also challenging to transform nonconductive microporous polymers into conductive microporous carbons while maintaining definite nanomorphology because the harsh carbonization conditions often give rise to the serious damage of nanomorphology.

On the other hand, hairy nanoparticles are an important class of nanomaterials composed of an inorganic/polymeric core and linear polymer chains grafted from/onto the core. They can be used as controlled release systems,[12] catalyst carriers,[13] plasmonic devices,[14] or electrode materials for energy storage.[15] The past few decades have witnessed the rapid growth in the area of hairy nanoparticles with various cores including silica nanospheres,[16] metal and metal oxide nanoparticles,[17] quantum dots,[18] and polymeric nanospheres.[1e,19] However, the hairy nanoparticles are essentially nonporous, except for a few unusual cases of mesoporous silica nanoparticles as the core.[16a] Therefore, it has been very difficult, if not impossible, to fabricate all-organic porous hairy nanoparticles, especially microporous ones.

Herein, for the first time, we report the design and fabrication of a novel class of water-dispersible, stimuli-responsive, and readily carbonizable hairy microporous polymeric nanospheres by the union of hyper-cross-linking chemistry and surface-initiated atom transfer radical polymerization (SI-ATRP). As shown in Figures 1 and S1, monodisperse poly(4-chloromethylstyrene) nanosphere with divinylbenzene (DVB) pre-cross-linking (PCMS) was initially prepared by surfactant-free emulsion polymerization and then was treated via a facile hyper-cross-linking procedure to provide the nanosphere with well-developed microporosity, thus obtaining microporous polymeric nanosphere (*x*PCMS). Then, hairy stimuli-responsive

Received: August 24, 2015
Published: October 1, 2015

DOI: 10.1021/jacs.5b08978
J. Am. Chem. Soc. 2015, 137, 13256−13259

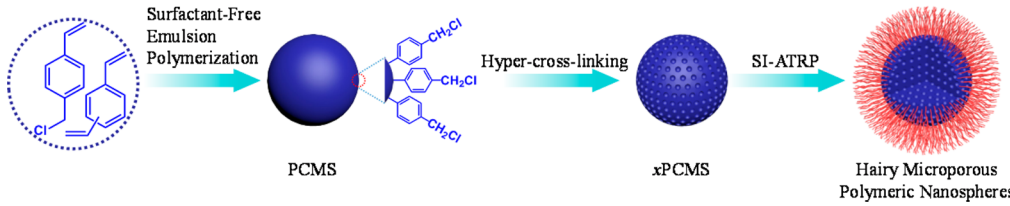

Figure 1. Schematic illustration for fabrication of water-dispersible, responsive, and carbonizable hairy microporous polymeric nanospheres.

hydrophilic polymeric blocks, such as pH/temperature dual-responsive hydrophilic poly(2-(dimethylamino)ethyl methacrylate) (PDMAEMA) and thermoresponsive poly(*N*-isopropylacrylamide) (PNIPAM), were grafted from *x*PCMS via SI-ATRP, leading to formation of the water-dispersible responsive hairy microporous polymeric nanospheres (e.g., *x*PCMS-*g*-PDMAEMA and *x*PCMS-*g*-PNIPAM). In this strategy, the choice of *x*PCMS is critical, because it plays two roles: (i) *x*PCMS has a high surface area of up to 1323 m^2 g^{-1}, which is vital to their potential use, e.g., gas storage, adsorption, or drug delivery; (ii) *x*PCMS contains many benzyl chloride initiating sites for SI-ATRP to introduce diverse hairy functional polymeric blocks (Table S1), which can bypass the complicated chlorine group modification process. The as-prepared hairy microporous polymeric nanospheres exhibit benign water-dispersibility, well-defined microporosity, and high surface area. They are sensitively responsive to pH/temperature and also demonstrate a much better adsorption capability toward water-soluble molecules as compared to original *x*PCMS. In addition, due to the hybrid of carbonizable core and thermo-decomposable protection shell, these hairy microporous polymeric nanospheres can be carbonized and can also effectively avoid intersphere thermofusion during carbonization, leading to formation of well-defined microporous carbon nanospheres.

PCMS was synthesized by surfactant-free emulsion polymerization of 4-chloromethylstyrene monomer and DVB precross-linker with 2,2′-azobis (2-amidinopropane) dihydrochloride as initiator. The hydrodynamic diameter (D_h) of PCMS in ethanol, as measured by dynamic light scattering (DLS) analysis, was 591 nm (Figure S2A), which was slightly larger than the diameter calculated by the SEM image (526 nm, Figures S2B and S3A). The DVB pre-cross-linking is necessary for PCMS. Normally, conventional PCMS nanospheres are fabricated by emulsion polymerization of 4-chloromethylstyrene. Such nanospheres without pre-cross-linking swell and dissolve in 1,2-dichloroethane solution during hyper-cross-linking, and their spherical shape would be seriously damaged or could even disappear. Consequently, DVB was used as a pre-cross-linker to obtain the pre-cross-linked PCMS, thus achieving the well-defined nanospherical morphology after hyper-cross-linking (Figure 2A). The nanosphere size increased to 540 nm for *x*PCMS (Figures 2A and S3B) and after surface grafting of PDMAEMA, to 568 nm for *x*PCMS-*g*-PDMAEMA (Figures 2B and S3C). Fourier transform infrared (FT-IR) spectra provided direct evidence of successful grafting of PDMAEMA chains from *x*PCMS, in which new adsorption peak around 1734 cm^{-1} corresponding to ester carbonyl band (C═O stretching vibrations) appeared after grafting (Figure S4). The elemental analysis showed that the nitrogen content for *x*PCMS-*g*-PDMAEMA was 1.69%, which could translate into a weight percentage of grafted PDMAEMA chains of 19.0%.

Nitrogen adsorption analysis was then used to track the evolution of pore structure during hyper-cross-linking and SI-ATRP (Figures 2C and S5). Before hyper-cross-linking, PCMS only adsorbed an extremely small quantity of nitrogen and presented a Brunauer–Emmett–Teller (BET) surface area as low as 11 m^2 g^{-1}, indicative of an essentially nonporous characteristic. In sharp contrast, after the hyper-cross-linking treatment, the resulting *x*PCMS exhibited a very steep rise in the nitrogen adsorption amount at low relative pressure (P/P_0), indicating generation of a well-developed microporous structure. This is because numerous $-CH_2-$ cross-linking bridges from $-CH_2Cl$ were introduced to subdivide the originally nonporous sphere space into a substantial number of micropores. Density functional theory (DFT) analysis showed these micropores were about 1.3 nm (Figure S5). Thus, *x*PCMS exhibited a very high BET surface area of 1323 m^2 g^{-1}. After grafting of nonporous PDMAEMA of 19.0% from the periphery of *x*PCMS, the diameter of micropores basically remained around 1.3 nm (the inset in Figure 2C), and a BET surface area as high as 562 m^2 g^{-1} was still retained. It should be noted that "grafting from" approach has already been a well-established method to synthesize polymer-grafted porous nanoobjects.[19b,20] However, the pore accessibility and specific surface areas were often sacrificed to a large extent. Interestingly, in the present case, most micropores were too small to allow for the polymer chain growth inside it via SI-ATRP, leading to the good preservation of microporosity after the surface grafting. Thus, the BET surface area for *x*PCMS-*g*-PDMAEMA was much higher than those for almost all reported polymer-grafted porous nanoobjects (normally 1.7–253 m^2 g^{-1}, Table S2).

In order to demonstrate the functionalization advantages for *x*PCMS-*g*-PDMAEMA, water-dispersibility tests of *x*PCMS and *x*PCMS-*g*-PDMAEMA were performed. As shown in Figure 3A,

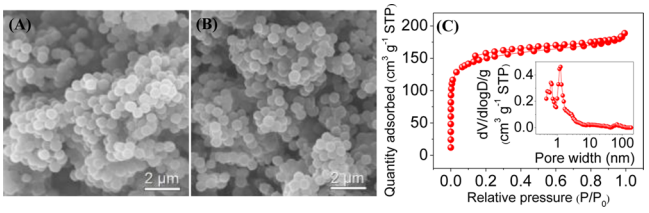

Figure 2. SEM images of (A) *x*PCMS and (B) *x*PCMS-*g*-PDMAEMA; (C) N_2 adsorption-desorption isotherm and DFT pore size distribution curve (the inset) for *x*PCMS-*g*-PDMAEMA.

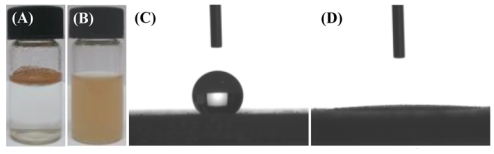

Figure 3. Water-dispersibility tests (0.3 mg mL^{-1}, stirring for 5 min) of (A) *x*PCMS and (B) *x*PCMS-*g*-PDMAEMA; and water contact angle measurements of (C) *x*PCMS and (D) *x*PCMS-*g*-PDMAEMA.

DOI: 10.1021/jacs.5b08978
J. Am. Chem. Soc. 2015, 137, 13256–13259

*x*PCMS failed to disperse in water and thus aggregated on the surface of water, due to their inherent hydrophobicity. In sharp contrast, after surface grafting of water-soluble PDMAEMA chains, *x*PCMS-*g*-PDMAEMA was hydrophilic and dispersed very well in water (Figure 3B). Water contact angle measurements (Figures 3C,D) further indicated that PCMS and *x*PCMS-*g*-PDMAEMA presented water contact angles of up to 142.0° and <5°, respectively, confirming the surface grafting-induced hydrophilicity.

The pH/temperature dual-responsive behavior for *x*PCMS-*g*-PDMAEMA was investigated by DLS measurements at different pH and temperatures, as shown in Figures 4 and S6. At pH 2,

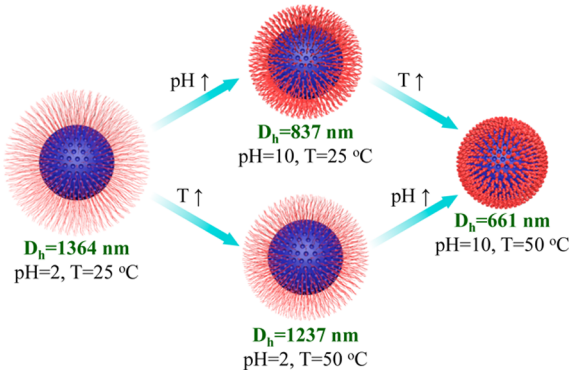

Figure 4. Hydrodynamic diameters of *x*PCMS-*g*-PDMAEMA (0.3 mg mL^{-1}) at different pH and temperatures, illustrating the pH/temperature dual-responsive behavior.

PDMAEMA chains were fully protonated and transformed into cationic polyelectrolytes. Due to the interchain electrostatic repulsion and good water affinity, PDMAEMA chains were swollen and showed large D_h = 1364 nm at 25 °C. However, when pH rose to 10, PDMAEMA chains were deprotonated, and their interchain interactions became stronger than chain−solvent interactions. As a result, *x*PCMS-*g*-PDMAEMA partially collapsed and D_h reduced to 837 nm at 25 °C. Moreover, D_h of *x*PCMS-*g*-PDMAEMA can be further decreased to 661 nm upon increasing the temperature to 50 °C. This transition is related to lower critical solution temperature (LCST) of nonprotonated PDMAEMA. However, lower pH = 2 at 50 °C swelled protonated PDMAEMA chains again leading to D_h = 1237 nm. Taken together, *x*PCMS-*g*-PDMAEMA demonstrated an interesting pH/temperature dual-responsive performance. Furthermore, *x*PCMS-*g*-PDMAEMA exhibited fast response kinetics; e.g., its D_h promptly decreased upon changing pH from 2 to 10 and immediately recovered upon decreasing pH to 2 again (Figure S7).

To further demonstrate the universality of this surface grafting-induced functionalization, we substituted the PDMAEMA with another thermoresponsive polymer, poly(*N*-isopropylacrylamide) (PNIPAM), thus producing *x*PCMS-*g*-PNIPAM. FT-IR spectrum of *x*PCMS-*g*-PNIPAM (Figure S8) showed new absorption peaks at 1653 and 1543 cm^{-1} corresponding to amide I band (C═O stretching) and amide II band (N−H stretching) after grafting. The as-prepared *x*PCMS-*g*-PNIPAM still had a high BET surface area of 595 m^2 g^{-1} (Figure S9), indicating good micropore preservation. The thermosensitive behavior was confirmed by DLS at different temperatures. For example, high D_h = 716 nm of *x*PCMS-*g*-PNIPAM at 20 °C, decreased to 614 nm at 40 °C, a temperature above the LCST of PNIPAM (Figure S10).

The adsorption properties in an aqueous phase for *x*PCMS-*g*-PDMAEMA were studied using water-soluble alizarin red as a model molecule. As shown in Figure 5A, *x*PCMS-*g*-PDMAEMA

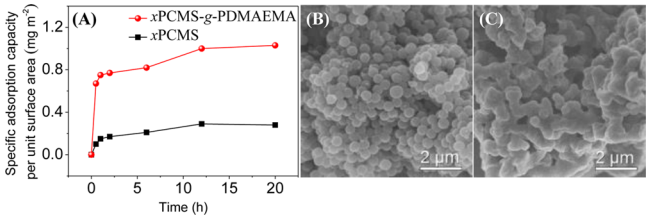

Figure 5. (A) Specific adsorption capacity per unit surface area toward alizarin red at 30 °C for *x*PCMS-*g*-PDMAEMA and *x*PCMS, showing the importance of good water-dispersibility for microporous polymer adsorbents in aqueous solution. SEM images of (B) C-*x*PCMS-*g*-PDMAEMA and (C) C-*x*PCMS, highlighting the importance of protection shell to nanomorphology stability during carbonization.

had a significantly higher specific adsorption capacity per unit surface area than *x*PCMS at various adsorption times. For example, *x*PCMS-*g*-PDMAEMA and *x*PCMS had 0.75 and 0.15 mg m^{-2} at 1 h, respectively, and had 1.03 and 0.28 mg m^{-2} at 20 h, respectively. This demonstrated that for *x*PCMS-*g*-PDMAEMA adsorption was much faster and had much more efficient pore surface utilization, probably because the water-dispersibility made the pores much more accessible to the adsorbates in the aqueous solution. Therefore, the alizarin red adsorption capacity of *x*PCMS-*g*-PDMAEMA was as high as 580 mg g^{-1}.

Porous carbon nanomaterials not only possess common characters of porous nanomaterials but also exhibit excellent conductive and electrochemical performances. They are used in many areas including energy, environment, adsorption, and catalysis. To fabricate porous carbons with well-defined nanostructures, one of the most common and effective routes is the pyrolysis of polymer precursors in inert atmosphere. However, during the pyrolysis treatment, fusion of polymeric nanostructure is generally inevitable, which makes it very difficult to obtain well-defined nanostructures for porous carbons.[21] Surprisingly, since *x*PCMS-*g*-PDMAEMA simultaneously contained carbonizable core and thermo-decomposable protection shell, *x*PCMS-*g*-PDMAEMA can be carbonized and can also effectively avoid intersphere fusion during carbonization. As a result, a novel class of well-defined carbon nanosphere with a highly microporous structure (C-*x*PCMS-*g*-PDMAEMA) by simple carbonization of *x*PCMS-*g*-PDMAEMA at 900 °C was produced. TGA measurement showed that PDMAEMA shell and *x*PCMS core started to degrade around 205 and 410 °C, respectively (Figure S11). SEM image of Figure 5B indicated that C-*x*PCMS-*g*-PDMAEMA preserved the uniform nanospherical morphology very well. Raman spectrum showed that C-*x*PCMS-*g*-PDMAEMA presented a graphite-like microcrystalline structure (Figure S12). Nitrogen adsorption measurement showed that C-*x*PCMS-*g*-PDMAEMA possessed numerous 0.5 nm micropores and had a high BET surface area of 908 m^2 g^{-1} (Figure S13). As a control, *x*PCMS was also carbonized under the same conditions. However, significant intersphere fusion occurred during the carbonization process, and thus the resulting C-*x*PCMS had a very ill-defined and irregular nanomorphology (Figure 5C). This comparison clearly confirmed that the protection of the sacrificial thermo-decomposable PDMAEMA shell is crucial to formation of the well-defined carbon nanomorphology.

DOI: 10.1021/jacs.5b08978
J. Am. Chem. Soc. 2015, 137, 13256−13259

In summary, we present a successful development of a novel class of water-dispersible, pH/temperature-responsive and readily carbonizable hairy microporous polymeric nanospheres based on the union of hyper-cross-linking and SI-ATRP. Microporous polymeric nanosphere *x*PCMS was first synthesized by hyper-cross-linking and then was directly used as initiating sites for SI-ATRP to introduce water-soluble and stimuli-responsive hairy polymeric grafts on the periphery of the nanosphere, including pH/temperature dual-responsive PDMAEMA and thermoresponsive PNIPAM. The as-prepared new hairy microporous polymeric nanospheres exhibited high surface areas because of the well-developed and preserved microporous structure in their hyper-cross-linked cores and displayed good water-dispersibility and valuable stimuli-responsiveness resulting from the water-soluble responsive hairy shells. The advanced microporous polymeric nanospheres also demonstrated excellent adsorption performance toward water-soluble molecules. Moreover, the unique hybrid of carbonizable core and thermo-decomposable protection shell made these new hairy nanoparticles an ideal precursor to well-defined microporous carbon nanospheres. We hope that this methodology will open a new door for design and fabrication of advanced multifunctional microporous nanoobjects and thus provide new opportunities for various areas including adsorption, separation, energy, catalysis and medicine.

■ ASSOCIATED CONTENT

Supporting Information

The Supporting Information is available free of charge on the ACS Publications website at DOI: 10.1021/jacs.5b08978.

Experimental details and other characterization data (PDF)

■ AUTHOR INFORMATION

Corresponding Authors

*wudc@mail.sysu.edu.cn

*km3b@andrew.cmu.edu

Notes

The authors declare no competing financial interest.

■ ACKNOWLEDGMENTS

This work was supported by the project of the National Natural Science Foundation of China (51422307, 51372280, 51173213, 51172290 and 51232005), Guangdong Natural Science Funds for Distinguished Young Scholar (S2013050014408), Program for New Century Excellent Talents in University by Ministry of Education (NCET-12-0572), Pearl River S&T Nova Program of Guangzhou (2013J2200015), Fundamental Research Funds for the Central Universities (15lgjc17, 13lgpy57), National Key Basic Research Program of China (2014CB932400), BSF (2012074), and NSF (DMR 1501324).

■ REFERENCES

(1) (a) Liang, Y.; Fu, R.; Wu, D. *ACS Nano* **2013**, *7*, 1748−1754. (b) Li, Z.; Wu, D.; Liang, Y.; Fu, R.; Matyjaszewski, K. *J. Am. Chem. Soc.* **2014**, *136*, 4805−4808. (c) Liang, Y.; Wu, D.; Fu, R. *Sci. Rep.* **2013**, *3*, 1119. (d) Su, D. S.; Perathoner, S.; Centi, G. *Chem. Rev.* **2013**, *113*, 5782−5816. (e) Wu, D.; Li, Z.; Zhong, M. J.; Kowalewski, T.; Matyjaszewski, K. *Angew. Chem., Int. Ed.* **2014**, *53*, 3957−3960. (f) Xu, F.; Tang, Z. W.; Huang, S. Q.; Chen, L. Y.; Liang, Y. R.; Mai, W. C.; Zhong, H.; Fu, R.; Wu, D. *Nat. Commun.* **2015**, *6*, 7221. (g) Wang, D.-W.; Li, F.; Liu, M.; Lu, G. Q.; Cheng, H.-M. *Angew. Chem.* **2008**, *120*, 379−282. (h) Yang, S. B.; Feng, X. L.; Zhi, L. J.; Cao, Q.; Maier, J.; Mullen, K. *Adv. Mater.* **2010**, *22*, 838−842.

(2) (a) Deng, X.; Mammen, L.; Zhao, Y.; Lellig, P.; Mullen, K.; Li, C.; Butt, H. J.; Vollmer, D. *Adv. Mater.* **2011**, *23*, 2962−2965. (b) Zhao, D. Y.; Feng, J.; Huo, Q.; Melosh, N.; Fredrickson, G. H.; Chmelka, B. F.; Stucky, G. D. *Science* **1998**, *279*, 548−552.

(3) Yang, P. D.; Zhao, D. Y.; Margolese, D. I.; Chmelka, B. F.; Stucky, G. D. *Nature* **1998**, *396*, 152−155.

(4) Li, H. L.; Eddaoudi, M.; O'Keeffe, M.; Yaghi, O. M. *Nature* **1999**, *402*, 276−279.

(5) (a) Furukawa, H.; Yaghi, O. M. *J. Am. Chem. Soc.* **2009**, *131*, 8875−8883. (b) Xu, F.; Xu, H.; Chen, X.; Wu, D.; Wu, Y.; Liu, H.; Gu, C.; Fu, R.; Jiang, D. L. *Angew. Chem., Int. Ed.* **2015**, *54*, 6814−6818. (c) Colson, J. W.; Woll, A. R.; Mukherjee, A.; Levendorf, M. P.; Spitler, E. L.; Shields, V. B.; Spencer, M. G.; Park, J.; Dichtel, W. R. *Science* **2011**, *332*, 228−231. (d) Feng, X.; Ding, X. S.; Jiang, D. L. *Chem. Soc. Rev.* **2012**, *41*, 6010−6022. (e) Xu, Y. H.; Jin, S. B.; Xu, H.; Nagai, A.; Jiang, D. L. *Chem. Soc. Rev.* **2013**, *42*, 8012−8031.

(6) (a) Johnson, S. A.; Ollivier, P. J.; Mallouk, T. E. *Science* **1999**, *283*, 963−965. (b) Xu, F.; Chen, X.; Tang, Z. W.; Wu, D.; Fu, R.; Jiang, D. L. *Chem. Commun.* **2014**, *50*, 4788−4790. (c) Li, Z.; Wu, D.; Huang, X.; Ma, J. H.; Liu, H.; Liang, Y.; Fu, R.; Matyjaszewski, K. *Energy Environ. Sci.* **2014**, *7*, 3006−3012. (d) Ouyang, Y.; Shi, H. M.; Fu, R.; Wu, D. *Sci. Rep.* **2013**, *3*, 1430. (e) Wu, D.; Hui, C. M.; Dong, H. C.; Pietrasik, J.; Ryu, H. J.; Li, Z.; Zhong, M. J.; He, H. K.; Kim, E. K.; Jaroniec, M.; Kowalewski, T.; Matyjaszewski, K. *Macromolecules* **2011**, *44*, 5846−5849. (f) Wu, D.; Xu, F.; Sun, B.; Fu, R.; He, H. K.; Matyjaszewski, K. *Chem. Rev.* **2012**, *112*, 3959−4015.

(7) (a) Xu, F.; Jin, S. B.; Zhong, H.; Wu, D.; Yang, X. Q.; Chen, X.; Wei, H.; Fu, R.; Jiang, D. L. *Sci. Rep.* **2015**, *5*, 8225. (b) Kou, Y.; Xu, Y. H.; Guo, Z. Q.; Jiang, D. L. *Angew. Chem., Int. Ed.* **2011**, *50*, 8753−8757.

(8) Wu, D.; Nese, A.; Pietrasik, J.; Liang, Y.; He, H. K.; Kruk, M.; Huang, L.; Kowalewski, T.; Matyjaszewski, K. *ACS Nano* **2012**, *6*, 6208−6214.

(9) Du, N. Y.; Robertson, G. P.; Song, J. S.; Pinnau, I.; Thomas, S.; Guiver, M. D. *Macromolecules* **2008**, *41*, 9656−9662.

(10) Abidian, M. R.; Kim, D. H.; Martin, D. C. *Adv. Mater.* **2006**, *18*, 405−409.

(11) Chan-Thaw, C. E.; Villa, A.; Katekomol, P.; Su, D. S.; Thomas, A.; Prati, L. *Nano Lett.* **2010**, *10*, 537−541.

(12) Zhang, Z.; Yin, L.; Tu, C.; Song, Z.; Zhang, Y.; Xu, Y.; Tong, R.; Zhou, Q.; Ren, J.; Cheng, J. *ACS Macro Lett.* **2013**, *2*, 40−44.

(13) Lu, Y.; Mei, Y.; Drechsler, M.; Ballauff, M. *Angew. Chem., Int. Ed.* **2006**, *45*, 813−816.

(14) Lupitskyy, R.; Motornov, M.; Minko, S. *Langmuir* **2008**, *24*, 8976−8980.

(15) Lin, H.-C.; Li, C.-C.; Lee, J.-T. *J. Power Sources* **2011**, *196*, 8098−8103.

(16) (a) Hong, C. Y.; Li, X.; Pan, C. Y. *J. Phys. Chem. C* **2008**, *112*, 15320−15324. (b) Tang, C.; Bombalski, L.; Kruk, M.; Jaroniec, M.; Matyjaszewski, K.; Kowalewski, T. *Adv. Mater.* **2008**, *20*, 1516−1522.

(17) Ohno, K.; Koh, K.; Tsujii, Y.; Fukuda, T. *Angew. Chem., Int. Ed.* **2003**, *42*, 2751−2754.

(18) Esteves, A. C. C.; Bombalski, L.; Trindade, T.; Matyjaszewski, K.; Barros-Timmons, A. *Small* **2007**, *3*, 1230−1236.

(19) (a) Fujii, S.; Kakigi, Y.; Suzaki, M.; Yusa, S.-I.; Muraoka, M.; Nakamura, Y. *J. Polym. Sci., Part A: Polym. Chem.* **2009**, *47*, 3431−3443. (b) Min, K.; Gao, H.; Yoon, J. A.; Wu, W.; Kowalewski, T.; Matyjaszewski, K. *Macromolecules* **2009**, *42*, 1597−1603.

(20) (a) Fu, Q.; Rao, G. V. R.; Ista, L. K.; Wu, Y.; Andrzejewski, B. P.; Sklar, L. A.; Ward, T. L.; Lopez, G. P. *Adv. Mater.* **2003**, *15*, 1262−1266. (b) Cao, L.; Man, T.; Zhuang, J.; Kruk, M. *J. Mater. Chem.* **2012**, *22*, 6939−6946. (c) Kruk, M.; Dufour, B.; Celer, E. B.; Kowalewski, T.; Jaroniec, M.; Matyjaszewski, K. *Macromolecules* **2008**, *41*, 8584−8591. (d) Luo, Z.; Cai, K.; Hu, Y.; Zhao, L.; Liu, P.; Duan, L.; Yang, W. *Angew. Chem., Int. Ed.* **2011**, *50*, 640−643. (e) Zhou, Z.; Zhu, S.; Zhang, D. *J. Mater. Chem.* **2007**, *17*, 2428−2438.

(21) Li, Z.; Wu, D.; Liang, Y.; Xu, F.; Fu, R. *Nanoscale* **2013**, *5*, 10824−10828.

DOI: 10.1021/jacs.5b08978
J. Am. Chem. Soc. 2015, 137, 13256−13259